Article

Investigating the Expression of Genes Involved in Apoptosis and Mutation in Ovarian Cancer Cell Line and Possible Hepatotoxicity in Rats Induced by New Green Synthesized Ag-NPs

Fang Fang,[a] Xiaoyan Zhang,[b] Rongrong Bai,[b] Bing Wang ⦿*,[c] and Mostafa Heidari Majd ⦿ [d]

[a]*Department of Gynecology, 3201 Hospital, 723000, Hanzhong, China*

[b]*Department of Obstetrics, Laoling People's Hospital, 253600, Dezhou City, China*

[c]*Department of Gynecology, Ankang Central Hospital, 725000, Ankang, China*

[d]*Department of Medicinal Chemistry, Faculty of Pharmacy, Zabol University of Medical Sciences, 9861615881, Zabol, Iran*

Silver nanoparticles (Ag-NPs) can enter tumor cells through endocytosis and transfer to mitochondria, then disrupt mitochondrial function, damage deoxyribonucleic acid (DNA), and finally lead to cell death and apoptosis. As the Ag-NPs synthesized by *Moringa peregrina* leaf extract contain biomolecules such as flavonoids and terpenoids, they may suppress cancer by disrupting the flow of autophagy and inhibiting the differentiation of cancer cells, especially in apoptosis-resistant cancer cells. Accordingly, the 3-(4,5-dimethylthiazol-2-yl)-2,5-diphenyltetrazoliumbromid (MTT) assay proved that Ag-NPs could inhibit the OVCAR-3 cell line in a time- and concentration-dependent manner. Real-time polymerase chain reaction (PCR) results showed that the ratio of the pro-apoptotic Bak1 gene to the anti-apoptotic Bclx gene increased about 10 times compared to the control. Also, the expression of the caspase-3 gene has increased about 18 times compared to the control. In addition, it was found that Ag-NPs can inhibit the progression of ovarian cancer cell lines and decrease the expression of the AKT1 gene by 0.08. And the more important point was the safety of Ag-NPs, which was checked by the lipid peroxidation method and it was confirmed that the treated hepatocytes did not have any significant difference in the production of malondialdehyde with the control and probably do not cause hepatotoxicity.

Keywords: *Moringa peregrina*, apoptosis, Bak1, AKT1, caspase-3, lipid peroxidation

Introduction

The use of medicinal plants in developed countries has received renewed attention and almost all countries are developing new therapeutic strategies based on their traditional herbal medicine. This renewed interest in traditional herbs may be accompanied by changes in the way of consumption or changes in the composition of herbal medicines to enhance the effect of natural products.[1] One of the new methods of using herbal medicines is the preparation of nanoparticles (NPs) using medicinal plants, which is known as the green synthesis of NPs.[2] Effective phytochemicals in plant organs, especially biological substances in leaves such as aldehydes, ketones, phenols, flavones, terpenoids, amides, and ascorbic and carboxylic acids can be widely used for the green synthesis of metal/metal oxide NPs, and investigated for utilize in biomedicine, catalysis, and optical imaging.[3]

In the meantime, the biosynthesis of silver NPs (Ag-NPs) by plants has received more attention because they have become known antimicrobial agents to reduce infections caused by surgery and can be used to heal wounds. In addition, Ag-NPs have anti-fungal, anti-inflammatory, anti-angiogenic, and anti-permeability activities.[4] Since silver is known to be a safe and effective metal for animal cells, new research has been directed toward its anticancer effects and induction of cell death in mammalian cells.[5]

It has been proven that Ag-NPs accumulate in endosomes after being uptake mainly by endocytosis and are then directed to lysosomal fusion. The acidic environment of the lysosome

*e-mail: Wangbing0117@outlook.com
Editor handled this article: Paulo Cezar Vieira

leads to an increase in the release of silver ions from Ag-NPs, and then they cause an imbalance in cellular homeostasis and finally apoptosis.[6] This type of action, in which the cytotoxic property of Ag-NPs appears only after their uptake by cells, is known as the "Trojan horse" mechanism.[5,7] On the other hand, biomolecules adsorbed onto Ag-NPs can affect intrinsic and extrinsic apoptotic pathways and change the expression of genes involved in apoptosis.[8] Therefore, we decided for the first time to synthesize the Ag-NPs using *Moringa peregrina* leaves extract and investigate its cytotoxic and apoptotic properties on ovarian cancer cells. *Moringa peregrina*, which is found in different regions of Asia and Africa, is rich in protein, polyphenol, flavonoid, isothiocyanate, glycoside, triterpenoid, and essential amino acids,[9] and therefore we expect it to be successful in positively changing the expression of genes involved in apoptosis. Also, in some circumstances, chemotherapeutic agents may provide temporary relief to cancer patients and promote tumor progression through chronic inflammation and/or suppression of antitumor immune responses.[10,11] Some studies[12] have proven that various natural bioactive compounds, especially phenolic compounds, have good inhibitory effects on cancer invasion and metastasis. For this reason, the ability of Ag-NPs to reduce AKT1 gene expression can indicate the inhibition of mutation in the OVCAR-3 cell line.

It has been proven that Ag-NPs with a size below 100 nm, in addition to inducing apoptosis, may cause oxidative stress, necrosis and degeneration of liver cells through an unknown mechanism.[13] Since the hydro-alcoholic extract of the leaves of *M. oleifera*, another *Moringa* species, had an antioxidant nature and was able to prevent acetaminophen-induced hepatotoxicity in rats,[14] we decided to demonstrate the superiority of Ag-NPs synthesized by this plant in inhibiting hepatotoxicity and investigate the possibility of oxidative deterioration using the lipid peroxidation method.

Experimental

Materials

All materials and solvents needed for this project were of high purity and were obtained from reputable companies. Ethanol and deionized water were purchased from Merck (Darmstadt, Germany). Silver nitrate (Ag-NO$_3$), 3-(4,5-dimethylthiazol-2-yl)-2,5-diphenyltetrazoliumbromid (MTT), trichloroacetic acid (TCA), and thiobarbituric acid (TBA) were obtained from Sigma-Aldrich (St. Louis, MO, USA). OVCAR-3 cells were purchased from the cell culture collection of Pasture Institute (Tehran, Iran, cat. No. C430). Phosphate-buffered saline (PBS) was purchased from Alfa Aesar (Massachusetts, United States). The materials required for cytotoxicity and apoptosis assay were all sterile and were purchased from reputable companies. RPMI-1640 medium was purchased from the Caisson labs (North Logan, UT, United States). Fetal bovine serum (FBS) and penicillin G-streptomycin were obtained from Gibco (Carlsbad, CA, United States). Two companies Roche (Rotkreuz, Switzerland) and Pars Tous (Mashhad, Iran) provided the High Pure RNA Isolation Kit and Easy™ cDNA Synthesis kit, respectively.

Preparation of hydro-alcoholic extract from *Moringa peregrina* leaves

First, the leaves of the *Moringa peregrina* were collected in the autumn season of 2021 from around the city of Iranshahr, Sistan, and Baluchistan province in the southeast of Iran. They were dried by lyophilization to preserve the bioactive compounds of the leaves. A specimen of the leaves was sent to the Herbarium of the Faculty of Pharmacy of Isfahan, Iran, for identification and was confirmed with the code 2025. For extract preparation of bioactive materials, 100 g fine powder of *Moringa peregrina* leaves was added to 250 mL of 80% v/v water/ethanol at room temperature in a 250 mL closed Erlenmeyer flask. The extraction process was done with an orbital shaker (200 rpm, 2 inches (5.1 cm) orbit diameter) for five days. The supernatant was separated using a Buchner vacuum funnel, and its ethanol was removed using a rotary evaporator (Heidolph, Schwabach, Germany). The aqueous extract was stored at −20 °C for further use.

Plant-mediated green synthesis of Ag-NPs

The green synthesis was done according to previously reported methods with some modifications.[2] For the reduction of Ag$^+$ ions, 90 mL aqueous solution of Ag-NO$_3$ (2 M) was prepared and then 10 mL of leaves extract was added slowly to the solution at 70 °C and stirred until a color change from yellow to dark brown was observed in the mixture. To precipitate Ag-NPs, the mixture was placed at 4 °C overnight and then collected by centrifugation. The drying operation was performed by a freeze dryer (Shimadzu, Kyoto, Japan) and the weight of the product was calculated as 8.9 g.

Investigating the characteristics of Ag-NPs

The surface morphologies of biosynthesized Ag-NPs were studied using a MIRA3 TESCAN field emission

scanning electron microscopy (FESEM) (Brno, Czech Republic), with an accelerating voltage of 5.0 kV. Of course, this device could measure the approximate size of the selected particles.[15] Also, using an energy dispersive X-ray spectroscopy (EDX or EDS) coupled in FESEM, the elemental composition of Ag-NPs was evaluated. The FTIR (Fourier transform infrared spectroscopy) spectra (Shimadzu, Kyoto, Japan) were obtained in the whole region of 4000 to 500 cm^{-1} to investigate and compare the parameters and functional groups of Ag-NPs and flower extract. And finally, to determine the surface charge of the colloidal solution of silver nanoparticles, the zeta potential was measured in the range of -200 mV to $+200$ mV using a Zetasizer device (Malvern, Caringbah, Australia).

In vitro MTT assay to measure cytotoxicity

OVCAR-3 cells were seeded for two weeks in 25 cm^2 cell culture flasks having RPMI-1640 medium supplemented with 10% FBS and 1% penicillin G-streptomycin. At appropriate times, the medium was completely removed and the cells were washed twice with PBS. Also, cell passage was performed for cell proliferation.[16] The cells at a density of 1.5×10^4 cells in the well were transferred into 96-well culture plates and incubated in a proper incubator overnight. In full compliance with sterile conditions, the OVCAR-3 human ovarian cancer cells were treated with five different concentrations of biosynthesized Ag-NPs (0.28 to 4.5 mg mL^{-1}) for 48 and 72 h. To create reproducibility and reduce error, each concentration was repeated four independent times (n = 4, ± standard deviation (SD)), and four wells were considered as negative controls for each period. After treatment, the media was carefully removed, then 150 μL of serum-free media and 50 μL of MTT in PBS were added to each well, and were incubated for an additional 4 h in dark at 37 ℃. Afterward, the supernatant was carefully discarded and the cells were rinsed with PBS (3 times). Subsequently, the water-insoluble formazan crystals were dissolved using 200 μL of an organic solvent such as dimethyl sulfoxide (DMSO) for spectroscopic analysis at 570 nm with a multi-well ELISA reader (Agilent BioTek 800; Santa Clara, California, United States).

Investigating the rate of apoptosis induction and cancer progression with real-time PCR method

OVCAR-3 cells were plated at a seeding density of 1.0×10^6 in T25 cm^2 flasks before overnight treatment with 1 mg mL^{-1} biosynthesized Ag-NPs. Also, an untreated flask was prepared as a control. After the treatment period, cells were washed (2 times with PBS), trypsinized, and centrifuged (2000 rpm × 4 min) to collect adherent cells. The cells were again centrifuged (3000 rpm, 5 min) and the pellet was re-suspended in 200 μL PBS. Other steps of ribonucleic acid (RNA) isolation were performed according to the manufacturer's protocol of the High Pure RNA Isolation Kit, which were fully described in our previous works.[17-19] Also, the details of complementary deoxyribonucleic acid (cDNA) synthesis according to the cDNA synthesis kit were mentioned in our previous work.[20] The expression of the genes listed in Table 1 was quantified using the Applied Biosystems StepOne™ instrument (Thermo Fisher Scientific, Massachusetts, USA) and according to the following thermal cycle: a holding stage at 95 °C for 12 min followed by 40 cycles of 95 °C for 20 s, 55 °C for 20 s and 72 °C for 20 s, and finally melt curve stage at 95 °C for 15 s, 60 °C for 60 s and 95 °C for 15 s. Each sample was assayed in duplicate, the average cycle threshold (CT) value was normalized to the housekeeping gene GAPDH (glyceraldehyde 3-phosphate dehydrogenase) and the fold change expression was calculated by the comparative CT (ΔΔCT) method.[17]

Table 1. Primer sequences designed for real-time polymerase chain reaction (PCR)

Gene	Primer sequence
AKT1	forward: CCAACACCTTCATCATCCGC reverse: AGTCCATCTCCTCCTCCTCC
Caspase-3	forward: TGCAGTCATTATGAGAGGCAAT reverse: AAGGTTTGAGCCTTTGACCA
Bclx	forward: TGGAAAGCGTAGACAAGGAGA reverse: TGCTGCATTGTTCCCATAGA
Bak1	forward: TCTGGGACCTCCTTAGCCCT reverse: AATGGGCTCTCACAAGGGTATT
GAPDH	forward: TTGCCATCAATGACCCCTTCA reverse: CGCCCCACTTGATTTTGGA

Estimation of lipid peroxidation

In the first step, hepatocytes were isolated from the liver a male Wistar rat using collagenase liver perfusion.[21] Rat (280 g) was obtained from the Beijing Vital River Laboratory Animal Technology Co., Ltd. (Beijing, China), and was kept in 3201 Hospital animal house (Hanzhong, China) approved by the China Association for Accreditation of Laboratory Animal Care (CNAS-CL06:2018) with a standard nutritional and environmental protocol under the principles of animal ethics. In the next step, the amount of malondialdehyde (MDA) generated during the lipid peroxidation process was measured to evaluate the level of probably oxidative stress induced by Ag-NPs. For this purpose, 1×10^6 hepatocytes mL^{-1} were treated for 3 h with 0, 1 and 2 mg mL^{-1} of biosynthesized Ag-NPs, separately.

J. Braz. Chem. Soc. **2024**, *35*, 1, e-20230105

3 of 8

Then, 250 μL of TCA (70%) and 500 μL of TBA (0.8%) were added to the cell suspensions and incubated for 40 min in a boiling water bath. After that, they were cooled in an ice bath for 5 min and finally centrifuged for 5 min at 8000 rpm. To determine the absorbance of pink chromogen (TBARS) produced during the oxidative stress process, 100 μL of the supernatant of each cell suspension was measured at 532 nm using UV-Vis spectrophotometer (Biochrom™ WPA Biowave II; Holliston MA, United States).

Results and Discussion

Investigating the characteristics of biosynthesized Ag-NPs

Two species of *Moringa* (*peregrina* and *oleifera*) are known as native medicinal plants in areas of India, southern Iran, western Asia such as Jordan, and Egypt, which are even used as food supplements.[14] It has been proven that their leaves are very nutritious and rich in minerals, protein, amino acids, and vitamins A, B, and C.[22] On the other hand, *Moringa peregrina* has good reducing agents, including flavonoids and phenolic acids,[23] which can facilitate the biosynthesis of NPs due to the presence of hydroxyl groups in their structure. Since there is little research about biosynthesized NPs from this plant, we decided to synthesize Ag-NPs with its leaf extract. The fact that the relatively high amount of flavonoids, carbohydrates, sapogenins, and steroids in plant extracts as reducing and covering agents can affect the stability of Ag-NPs have been proven. These synthesized NPs have an average size below 100 nm and are spherical in shape.[24] Considering the use of room temperature for the preparation of *Moringa peregrina* leaf extract and maintaining the active biomolecules with this method, we expect the size of the synthesized NPs to be in a suitable range. Accordingly, size measurement and

morphological analysis by FESEM showed that Ag-NPs were spherical and their average size in solid state was ca. 87 nm (Figure 1a).

During the formation of metallic NPs using plant extract as a reducing agent, the biomolecules can adsorb on their surface due to high surface compatibility.[25] This fact was well confirmed by EDX analysis (Figure 1b) because, in addition to the presence of Ag in the spectrum, the observed C and O molecules confirmed the presence of surface-adsorbed biomolecules. Another interesting point was the appearance of peaks related to Ca and Mg in the EDX spectrum, which was in line with the results of ionic liquid chromatography analysis conducted by Al Juhaimi *et al.*[14] The appearance of the Au element was due to the coating of the green NPs during FESEM imaging to obtain a high-resolution image and prevent the charging of non-conductive biological samples.[26]

By comparing two FTIR spectra related to *Moringa peregrina* leaf extract and biosynthesized Ag-NPs together, it was possible to understand the correctness of the synthesis (Figure 2). So that the presence of different functional groups related to plant extract can be observed in the structure of nanoparticles. For example, the specified region (*i*) corresponded to the hydroxyl (−OH) groups of active molecules observed in Ag-NPs spectra with less intensity, the specified region (*ii*) related to methylene groups (CH_2) asymmetric stretching vibrations, the specified region (*iii*) belonged to the stretching vibration of the C=O bonds which observed in Ag-NPs spectra with high intensity, the specified region (*iv*) corresponded to the carbon-carbon double (C=C) bonds, and the specified region (*v*) associated with the CH_2 bending and CH_2 wagging modes. Additionally, the sharp peak at fingerprint region (*vi*) proves the existence and synthesis of Ag-NPs.

Ag-NPs have high amounts of surface charges (zeta potential), which are caused by the surface adsorption of
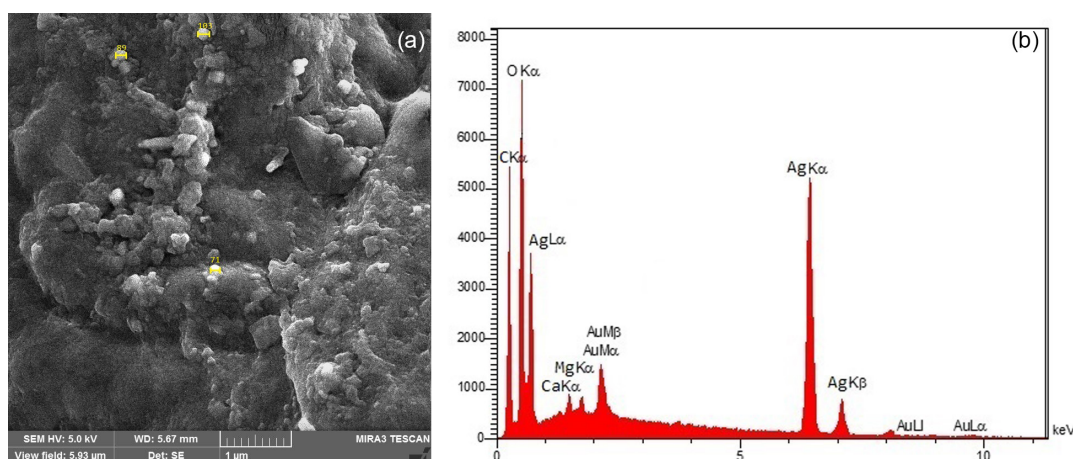

Figure 1. (a) The FESEM image of Ag-NPs and (b) EDX diagram used for the elemental analysis of Ag-NPs.
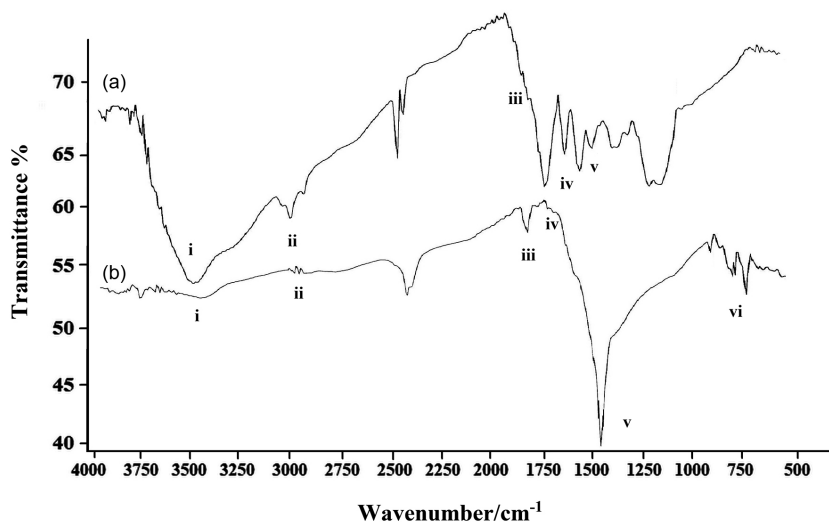
Figure 2. FTIR spectra of (a) *Moringa peregrina* leaf extract and (b) biosynthesized Ag-NPs. The samples were prepared for IR spectroscopy as KBr disks.

biomolecules available in the plant extract. These surface charges create repulsion in the suspension, so the greater the repulsion force between the particles, the greater the physical stability of the colloids and the less aggregation.[27] On the other hand, the zeta potential is the main factor in the initial absorption of NPs on the cell membrane and can affect endocytosis and cytotoxicity.[28] For these reasons, zeta potential was measured according to the usual method by a Malvern Zetasizer_nanoZS and its value was found to be −23 mV. This is the best size that can ensure the physiological stability and cytotoxic properties of biosynthesized Ag-NPs.

Cytotoxic study on OVCAR-3 cells by MTT assay

Ag-NPs can enter tumor cells through diffusion, phagocytosis, or endocytosis, bind to the outer membrane of cells, act as sustained-release extracellular drug carriers, or transport to mitochondria, cytoplasm, nucleus, and vesicles, then weaken the antioxidant defense function of cells, disturb the role of mitochondria, damage DNA and finally lead to cell death and apoptosis.[29] Of course, the biomolecules in plant extracts, which were used as reducing agents for biosynthesis of NPs, also play an important role in the biological activity of Ag-NPs.[30] Since *Moringa peregrina* leaves contain significant amounts of flavonoids and terpenoids, we can hope for a positive effect of silver nanoparticles on cancer. It has been proven that flavonoids have the ability to suppress cancer by stimulating autophagy or disrupting the autophagy flux, especially in apoptosis-resistant cancer cells.[31] Also, the role of terpenoids in suppressing the early stage of tumorigenesis by inducing cell cycle arrest and inhibiting the differentiation of cancer cells has been well confirmed.[32]

In a study conducted by Mansour *et al.*,[33] it was found that the *Moringa peregrina* leaves extract extracted by diethyl ether and ethyl acetate solvents can show good anticancer activity on hepatocellular carcinoma (HepG2) and breast carcinoma (MCF-7) cell lines. Also, they proved that the extracts cause little toxicity in normal melanocytes cell line HFB4.[33] On the other hand, there is only one valid report of concentration-dependent effects of Ag-NPs synthesized by *Moringa oleifera* leaves extract, another species of *Moringa* plant, on A375 human melanoma cells.[34] Therefore, we decided for the first time to investigate the cytotoxic effects of Ag-NPs synthesized by *Moringa peregrina* leaves extract on human ovarian adenocarcinoma cell lines (OVCAR-3) using the MTT method.

In Figure 3, it is evident that Ag-NPs were able to inhibit the proliferation of cancer cells from a concentration of 0.56 mg mL^{-1} and higher, and reduce the viability of cancer cells to about 13% after 72 h of exposure compared to the control. In other words, a concentration lower
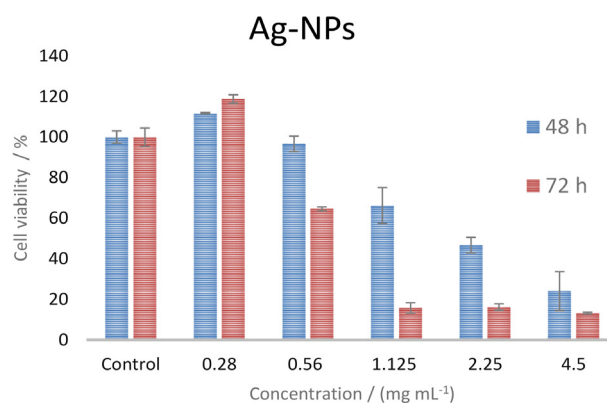

Figure 3. The anti-ovarian cancer properties (cell viability (%)) of Ag-NPs (concentrations of 0.28-4.5 mg mL^{-1}) against OVCAR-3 cell lines after 48 and 72 h incubation.

J. Braz. Chem. Soc. **2024**, *35*, 1, e-20230105

5 of 8

than 0.3 mg mL^{-1} cannot show any anti-ovarian cancer properties. The effect depending on the concentration and time of Ag-NPs was evident from the graphs and IC$_{50}$ (concentration with 50% inhibition) values (2 and 0.9 mg mL^{-1} related to 48 and 72 h incubation, respectively).

Examining the gene pathways of apoptosis and cancer mutation by real-time PCR

The first pathway of apoptosis, which is known as the extrinsic pathway, occurs through cell surface proteins and activates caspases 8 and 10, which subsequently activate effector caspases (3, 6, and 7) and causes the release of cytochrome C in the cytoplasm.[35,36] Also, the release of cytochrome C from the mitochondrial intermembrane space is the main reason for the activation of the intrinsic apoptosis pathway (the mitochondrial pathway), which depends on many stimuli such as oxidative stress, radiation, cytotoxic drugs, deoxyribonucleic acid (DNA) damage, and hypoxia.[37,38] Bcl-2 family members are key regulators of the intrinsic pathway of apoptotic cell death. This family consists of two groups of proteins with opposite activities in the process of apoptosis. Pro-apoptotic proteins such as Bax, Bak, Bad, Bcl-Xs, Bid, Bik, Bim, and Hrk cause the release of cytochrome C by forming pores in the mitochondrial membrane, while anti-apoptotic proteins such as Bcl-2, Bcl-xL, Bcl-W, Bfl-1, and Mcl-1 act oppositely and prevent the release.[39]

Examination of HepG2 cells treated with *Moringa peregrina* leaves extract confirmed that the bioactive compounds from the ethyl acetate extracts could increase the expression of BAX and caspase-3 genes, while the expression of the BCL-2 gene was decreased.[33] Therefore, it was necessary to investigate the possible pathways of apoptosis such as Bak1, Bclx, and Caspase-3 induced by Ag-NPs and their expression levels. This was the first study in which Ag-NPs biosynthesized with the *Moringa peregrina* leaves extract was used for the treatment of cancer cells. Also, the expression of routine genes specifying apoptosis was investigated, because these Ag-NPs carry surface adsorption biomolecules that may play a role in apoptosis.

As we expected, due to the presence of active biomolecules, the Ag-NPs were able to activate the mitochondrial pathway of apoptosis (intrinsic pathway) and increase the expression of the pro-apoptotic gene Bak1 by 2.988 times the control, and on the contrary, decrease the expression of the anti-apoptotic gene Bclx by 0.303 times the control (Figure 4). Based on this, the Bak1/Bclx ratio was calculated to be 9.86, which can be considered as an indicator of apoptosis induction by Ag-NPs in OVCAR-3 cell line (Table 2).
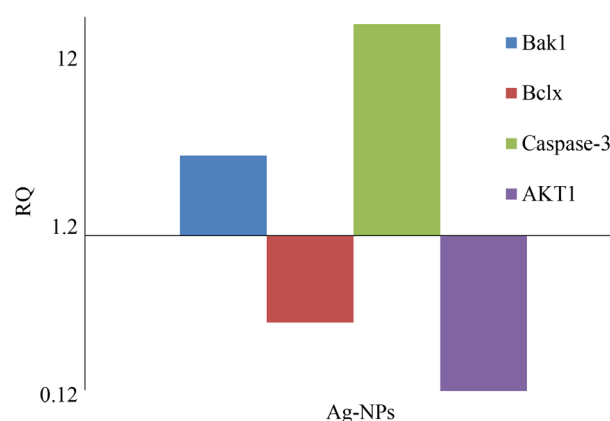

Figure 4. The expression level of genes involved in apoptosis and cancer mutation in OVCAR-3 cell line. The graph is drawn according to RQ (relative quantification) which is equal with $2^{(-\Delta\Delta CT)}$.

Caspase-3 is the most important caspase and can be activated through extrinsic and intrinsic pathways. It has also been proven that mitochondria can act as enhancers of caspase activities.[40] This fact is in line with the real-

Table 2. Evaluation of genes expression involved in apoptosis and cancer mutation stimulated by Ag-NPs biosynthesized by *Moringa peregrina* plant extract. RQ is equal with $2^{(-\Delta\Delta CT)}$

Gene	Sample	CT (mean)	ΔCT	ΔΔCT	RQ
AKT1	control	23.6113	4.5253	0	1
	Ag-NPs	33.7983	8.0627	3.5374	0.0861
Bak1	control	26.1379	7.0518	0	1
	Ag-NPs	31.2083	5.4727	−1.5791	2.988
Bclx	control	15.5125	−3.5735	0	1
	Ag-NPs	23.8825	−1.8531	1.7204	0.303
Caspase-3	control	30.9565	11.8704	0	1
	Ag-NPs	33.4301	7.6945	−4.1759	18.074
GAPDH	control	19.086			
	Ag-NPs	25.7356			

GAPDH is endogenous control and used to normalize the gene expression data. RQ: relative quantification; CT: cycle threshold; ΔΔCT: comparative cycle threshold.

time PCR results for caspase-3 and the Ag-NPs were able to increase their expression by 18.074 times the control (Table 2). On the other hand, as a new measure, we tried to check the level of AKT1 protein expression, because AKT activation is common in high-grade and late-stage serous ovarian carcinomas and may play a role in the progression of these tumors. Therefore, selective inhibition of AKT1 is required for maximal antitumor effects in ovarian cancer cell lines to prevent cancer mutation.[41] The results of Figure 4 show that the expression of the AKT1 gene is greatly reduced (0.0861) and it confirms that Ag-NPs biosynthesized by *Moringa peregrina* leaf extract can inhibit cancer progression and prevent its mutation. Therefore, we can hope for anti-cancer, apoptotic, and anti-mutation effects of Ag-NPs.

Estimation of lipid peroxidation

After targeted or non-targeted entry, Ag-NPs can accumulate in various tissues, including the heart, liver, kidney, lung, and nerve tissues, where they may interfere with the function of normal cells and cause adverse effects and toxicity.[42] In a research conducted by Albrahim *et al.*,[43] it was confirmed that toxication with Ag-NPs caused significant damage in renal DNA, increased lipid peroxidation, and decreased activity of superoxide dismutase, glutathione, and catalase in kidney tissue. On the other hand, Yousef *et al.*[44] confirmed that long-term exposure to Ag-NPs in male rats will cause cardiotoxicity and lung toxicity, so the toxic effects may be caused by the induction of lipid peroxidation and oxidative DNA damage.

The liver is especially the place of accumulation of Ag-NPs, so the release of silver ions and the formation of reactive oxygen species (ROS) can cause oxidative stress and subsequent lipid peroxidation and finally lead to the death of hepatocytes.[45] Several studies[46,47] reported that the liver and kidneys are the main tissues for the accumulation of Ag-NPs in rats after intravenous injection as well as oral consumption, so the accumulation leads to damage in those tissues, inflammation and oxidative stress. Therefore, evaluating the level of the MDA as an index for lipid peroxidation induced in isolated hepatocytes of rats was useful to understand the safety of Ag-NPs.

For this purpose, hepatocytes were isolated from rat liver and *in vitro* exposed to Ag-NPs synthesized by *Moringa peregrina* leaves extract. The results of Figure 5 showed that the differences between the control and treatment groups (1 and 2 mg mL^{-1} of Ag-NPs obtained from the IC$_{50}$ values) are not statistically significant ($P \leq 0.05$), and the formation of MDA in the hepatocytes in all culture media during the lipid peroxidation assay

was almost equal. Our results confirm the fact that the hydro-alcoholic extract of *M. oleifera* leaves, another *Moringa* species, has antioxidant nature and can prevent acetaminophen-induced hepatotoxicity in rats.[14]
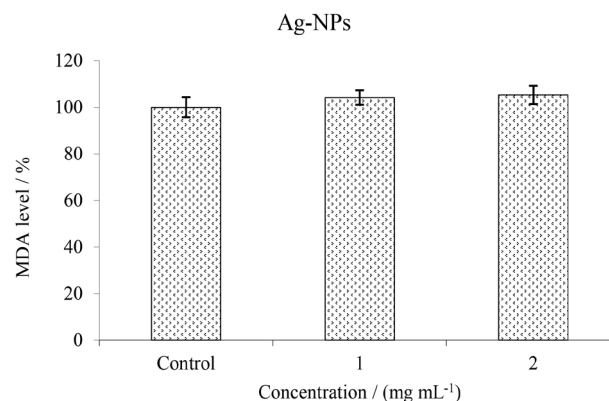

Figure 5. Levels of MDA formed during lipid peroxidation assay by hepatocytes isolated from rat liver.

Conclusions

In this research, silver nanoparticles (Ag-NPs) with an average size of about ca. 87 nm were synthesized by *Moringa peregrina* leaves extract and it was proved by EDX analysis that active biomolecules plus metals such as Ca and Mg were adsorbed on the surface of the nanoparticles. Since Ag-NPs synthesized by *Moringa peregrina* leaves extract contain biomolecules such as flavonoids and terpenoids, they were able to exert good cytotoxic and apoptotic effects on Bak1, Bclx, and caspase-3 genes. In addition, it was found that Ag-NPs can prevent the progression and mutation of ovarian cancer cell lines (OVCAR-3). And finally, it was proved that the treated hepatocytes do not have a significant difference in the production of malondialdehyde with the control, and probably the use of Ag-NPs does not lead to hepatotoxicity in patients.

Acknowledgments

References

1. Sánchez, M.; González-Burgos, E.; Iglesias, I.; Lozano, R.; Gómez-Serranillos, M. P.; *BMC Complementary Med. Ther.* **2020**, *20*, 306. [Crossref]

2. Yan, M.; Majd, M. H.; *Dokl. Biochem. Biophys.* **2021**, *500*, 360. [Crossref]

J. Braz. Chem. Soc. **2024**, *35*, 1, e-20230105

7 of 8

3. Singh, J.; Dutta, T.; Kim, K.-H.; Rawat, M.; Samddar, P.; Kumar, P.; *J. Nanobiotechnol.* **2018**, *16*, 84. [Crossref]

4. Keat, C. L.; Aziz, A.; Eid, A. M.; Elmarzugi, N. A.; *Bioresour. Bioprocess.* **2015**, *2*, 47. [Crossref]

5. Kovács, D.; Igaz, N.; Gopisetty, M. K.; Kiricsi, M.; *Int. J. Mol. Sci.* **2022**, *23*, 839. [Crossref]

6. Cameron, S. J.; Hosseinian, F.; Willmore, W. G.; *Int. J. Mol. Sci.* **2018**, *19*, 2030. [Crossref]

7. Hsiao, I. L.; Hsieh, Y.-K.; Wang, C.-F.; Chen, I. C.; Huang, Y.-J.; *Environ. Sci. Technol.* **2015**, *49*, 3813. [Crossref]

8. Yuan, Y. G.; Zhang, S.; Hwang, J. Y.; Kong, I. K.; *Oxid. Med. Cell. Longevity* **2018**, *2018*, 6121328. [Crossref]

9. Al-Qaraleh, S. Y.; Al-Zereini, W. A.; Oran, S. A.; Al-Sarayreh, A. Z.; Al-Dalain, S. M.; *OpenNano* **2022**, *8*, 100109. [Crossref]

10. Fan, Y.; Shen, B.; Tan, M.; Mu, X.; Qin, Y.; Zhang, F.; Liu, Y.; *FEBS J.* **2014**, *281*, 1750. [Crossref]

11. Lu, L.; Xu, X.; Zhang, B.; Zhang, R.; Ji, H.; Wang, X.; *J. Transl. Med.* **2014**, *12*, 36. [Crossref]

12. Subramaniam, S.; Selvaduray, K. R.; Radhakrishnan, A. K.; *Biomolecules* **2019**, *9*, 758. [Crossref]

13. Arora, S.; Jain, J.; Rajwade, J. M.; Paknikar, K. M.; *Toxicol. Lett.* **2008**, *179*, 93. [Crossref]

14. Al Juhaimi, F.; Ghafoor, K.; Ahmed, I. A. M.; Babiker, E. E.; Özcan, M. M.; *J. Food Meas. Charact.* **2017**, *11*, 1745. [Crossref]

15. Dou, J.; Mi, Y.; Daneshmand, S.; Heidari Majd, M.; *Arabian J. Chem.* **2022**, *15*, 104307. [Crossref]

16. Shahraki, S.; Shiri, F.; Heidari Majd, M.; Dahmardeh, S.; *J. Biomol. Struct.* **2019**, *37*, 2072. [Crossref]

17. Sargazi, A.; Barani, A.; Heidari Majd, M.; *BioNanoScience* **2020**, *10*, 683. [Crossref]

18. Habibi Khorassani, S. M.; Ghodsi, F.; Arezomandan, H.; Shahraki, M.; Omidikia, N.; Hashemzaei, M.; Heidari Majd, M.; *BioNanoScience* **2021**, *11*, 667. [Crossref]

19. He, C.; Heidari Majd, M.; Shiri, F.; Shahraki, S.; *J. Mol. Struct.* **2021**, *1229*, 129806. [Crossref]

20. Majd, M. H.; *Tumor Discovery* **2022**, *1*, 41. [Crossref]

21. Ou, X.; Shahraki, J.; Heidari Majd, M.; *Lat. Am. J. Pharm.* **2021**, *40*, 2219. [Crossref]

22. Sreelatha, S.; Jeyachitra, A.; Padma, P. R.; *Food Chem. Toxicol.* **2011**, *49*, 1270. [Crossref]

23. Soliman, A. S.; El-feky, S. A.; Darwish, E.; *J. Hortic. For.* **2015**, *7*, 36. [Crossref]

24. Ahmed, S.; Ahmad, M.; Swami, B. L.; Ikram, S.; *J. Adv. Res.* **2016**, *7*, 17. [Crossref]

25. Ying, S.; Guan, Z.; Ofoegbu, P. C.; Clubb, P.; Rico, C.; He, F.; Hong, J.; *Environ. Technol. Innov.* **2022**, *26*, 102336. [Crossref]

26. Park, J. B.; Kim, Y.-J.; Kim, S.-M.; Yoo, J. M.; Kim, Y.; Gorbachev, R.; Barbolina, I.; Kim, S. J.; Kang, S.; Yoon, M.-H.; *2D Materials* **2016**, *3*, 045004. [Crossref]

27. Marathe, S.; Shadambikar, G.; Mehraj, T.; Sulochana, S. P.; Dudhipala, N.; Majumdar, S.; *Pharmaceutics* **2022**, *14*, 1034. [Crossref]

28. Rasmussen, M. K.; Pedersen, J. N.; Marie, R.; *Nat. Commun.* **2020**, *11*, 2337. [Crossref]

29. Raja, G.; Jang, Y. K.; Suh, J. S.; Kim, H. S.; Ahn, S. H.; Kim, T. J.; *Cancers* **2020**, *12*, 664. [Crossref]

30. Poudel, D. K.; Niraula, P.; Aryal, H.; Budhathoki, B.; Phuyal, S.; Marahatha, R.; Subedi, K.; *J. Nanotechnol.* **2022**, *2022*, ID 2779237. [Crossref]

31. Zhang, Z.; Shi, J.; Nice, E. C.; Huang, C.; Shi, Z.; *Antioxidants* **2021**, *10*, 1138. [Crossref]

32. Kamran, S.; Sinniah, A.; Abdulghani, M. A. M.; Alshawsh, M. A.; *Cancers* **2022**, *14*, 1100. [Crossref]

33. Mansour, M.; Mohamed, M. F.; Elhalwagi, A.; El-Itriby, H. A.; Shawki, H. H.; Abdelhamid, I. A.; *BioMed. Res. Int.* **2019**, *2019*, 2698570. [Crossref]

34. Mohammed, G. M.; Hawar, S. N.; *Int. J. Biomater.* **2022**, *2022*, ID 4136641. [Crossref]

35. Jin, Z.; El-Deiry, W. S.; *Cancer Biol. Ther.* **2005**, *4*, 147. [Crossref]

36. Billen, L. P.; Shamas-Din, A.; Andrews, D. W.; *Oncogene* **2008**, *27*, S93. [Crossref]

37. Zhang, J.; Yu, Q.; Han, L.; Chen, C.; Li, H.; Han, G.; *Apoptosis* **2017**, *22*, 777. [Crossref]

38. Loreto, C.; La Rocca, G.; Anzalone, R.; Caltabiano, R.; Vespasiani, G.; Castorina, S.; Ralph, D. J.; Cellek, S.; Musumeci, G.; Giunta, S.; Djinovic, R.; Basic, D.; Sansalone, S.; *Biomed. Res. Int.* **2014**, *2014*, ID 616149. [Crossref]

39. Opferman, J. T.; Kothari, A.; *Cell Death Differ.* **2018**, *25*, 37. [Crossref]

40. Seervi, M.; Xue, D.; *Curr. Top. Dev. Biol.* **2015**, *114*, 43. [Crossref]

41. Hanrahan, A. J.; Schultz, N.; Westfal, M. L.; Sakr, R. A.; Giri, D. D.; Scarperi, S.; Janakiraman, M.; Olvera, N.; Stevens, E. V.; She, Q. B.; Aghajanian, C.; King, T. A.; Stanchina, E.; Spriggs, D. R.; Heguy, A.; Taylor, B. S.; Sander, C.; Rosen, N.; Levine, D. A.; Solit, D. B.; *Cancer Discov.* **2012**, *2*, 56. [Crossref]

42. Ferdous, Z.; Nemmar, A.; *Int. J. Mol. Sci.* **2020**, *21*, 2375. [Crossref]

43. Albrahim, T.; *Environ. Sci. Pollut. Res. Int.* **2020**, *27*, 38871. [Crossref]

44. Yousef, M. I.; Abuzreda, A. A.; Kamel, M. A.; *Exp. Ther. Med.* **2019**, *18*, 4329. [Crossref]

45. Yousef, H. N.; Ibraheim, S. S.; Ramadan, R. A.; Aboelwafa, H. R.; *Oxid. Med. Cell. Longev.* **2022**, *2022*, ID 3820848. [Crossref]

46. Su, C.-K.; Liu, H.-T.; Hsia, S.-C.; Sun, Y.-C.; *Anal. Chem.* **2014**, *86*, 8267. [Crossref]

47. Tiwari, D. K.; Jin, T.; Behari, J.; *Toxicol. Mech. Methods* **2011**, *21*, 13. [Crossref]